Available online at www.sciencedirect.com

ScienceDirect

Developmental Biology 312 (2007) 501 – 508

DEVELOPMENTAL BIOLOGY

www.elsevier.com/developmentalbiology

Disruption of the ubiquitin ligase *HERC4* causes defects in spermatozoon maturation and impaired fertility

Clara I. Rodriguez [1], Colin L. Stewart *

Cancer and Developmental Biology Laboratory, National Cancer Institute, Division of Basic Science, National Cancer Institute at Frederick, Frederick, MD 21702, USA

Received for publication 1 May 2007; revised 24 September 2007; accepted 25 September 2007
Available online 4 October 2007

Abstract

Spermatogenesis in mammals necessitates an extensive remodeling and loss of many cellular organelles and proteins as the spermatozoa undergo maturation. The removal of proteins and organelles depends on the ubiquitin–proteasome pathway. Here we show that the E3 ubiquitin ligase *Herc4*, though ubiquitously expressed in all tissues, is most highly expressed in the testis, specifically during spermiogenesis. Mice homozygous for a *Herc4* mutation are overtly normal; however, overall the males produce litter sizes some 50% smaller whereas female homozygotes show normal fertility. The reduced fertility in males is associated with about 50% of mature spermatozoa having reduced motility. Many of the spermatozoa possess an angulated tail with a cytoplasmic droplet being retained at the angulation. Our results show that *Herc4* ligase is required for proper maturation and removal of the cytoplasmic droplet for the spermatozoon to become fully functional.
Published by Elsevier Inc.

Keywords: *HERC4*; *HERC* family; E3 ubiquitin ligase; Spermatogenesis; Male fertility defect

Introduction

Spermatogenesis is a complex process of differentiation during which stem cell spermatogonia are transformed into highly differentiated spermatids through three phases (de Kretser et al., 1998). In the proliferative phase, spermatogonia undergo successive mitotic divisions; in the meiotic phase, spermatogonia are transformed into spermatocytes in which the genetic material undergoes homologous recombination and two sequential cell divisions, resulting in haploid spermatids. The last phase is spermiogenesis, in which the round haploid spermatids differentiate into elongated spermatids that are released into the seminiferous lumen. They then progress to the epididymis where they undergo further maturation and acquire the ability to fertilize an egg following a subsequent period of capacitation in the female reproductive tract. During spermiogenesis, each immature spermatid develops an acrosome, a tail, reorganizes its mitochondria, and loses most of its cytoplasm. Many proteins and organelles are removed in a residual body (RD), which is phagocytosed by adjacent Sertoli cells (Russell and Clermont, 1976). However, the specific mechanisms by which the cytoplasmic volume is reduced and organelle removal occurs to generate the residual body remain unclear. Recent evidence indicates that the ubiquitin–proteosome system plays a role in this developmental process (Sutovsky, 2003).

Ubiquitination of proteins is performed by a series of enzymatic steps involving an E1 ubiquitin-activating enzyme, an E2 ubiquitin conjugase, and an E3 ubiquitin ligase (Hershko et al., 2000; Weissman, 2001; Wilkinson, 2000). Although there is only one E1 enzyme and a limited number of E2 enzymes, ubiquitin ligases are abundant and bind both the E2 enzyme and a specific substrate to ensure specific substrate recognition. Polyubiquitinated proteins are translocated to the proteasome and degraded in an energy-dependent manner. The ubiquitin–proteasome pathway plays important roles in regulating protein turnover in numerous cellular processes, including the degradation of intracellular proteins, cell-cycle regulation, stress

* Corresponding author. Present address: Institute of Medical Biology, 8A Biomedical Grove #06-06 Immunos Singapore 138648. Fax: +65 6464 2049.
E-mail address: colin.stewart@imb.a-star.edu.sg (C.L. Stewart).
[1] Present address: Stem Cell Laboratory, Endocrinology and Diabetes Research Group, Hospital de Cruces, Barakaldo, Bizkaia, 48903 Spain.

0012-1606/$ - see front matter. Published by Elsevier Inc.
doi:10.1016/j.ydbio.2007.09.053

responses, and programmed cell death (Baarends et al., 1999; Ciechanover et al., 2000; Varshavsky, 2005; Wilkinson, 2000).

Three groups of E3 enzymes, HECT (homologous to E6AP (E6-associated protein) C-terminus), RING, and U-box proteins, have been identified and each is defined by its mode of action and the structure of their catalytic sites. Among the E6AP ligases, the presence of both HECT and RCC1-like domains categorize a sub-family of proteins referred to as HERC proteins as defined by the Human Genome Organization (Ji et al., 1999). HECT domains show approximately 50% similarity to the carboxyl-terminal region of E6-associated protein (E6AP). The ubiquitin ligase activity of E6AP functions not only in pathological conditions, for example the E6–E6AP complex functions as a ubiquitin ligase for p53 (Scheffner et al., 1993), but also in physiological pathways in which proteins other than p53 undergo E6AP-mediated ubiquitination (Kuhne and Banks, 1998; Kumar et al., 1999; Oda et al., 1999). The RCC1-like domain, or RLD, is a structural motif displaying high similarity to the sequence of the RCC1 protein (regulator of *c*hromosome *c*ondensation-1). RCC1 is a guanine nucleotide exchange factor for G proteins which participates in nucleocytoplasmic transport and is characterized by several repeats of 51–68 amino acids each, resulting in a domain of up to 400 residues (Garcia-Gonzalo and Rosa, 2005).

The human HERC family of proteins is composed of six members and all contain one or more RLDs upstream of a HECT domain. In mice, only five members have been identified (Garcia-Gonzalo and Rosa, 2005). Most HERC proteins are ubiquitously expressed, with higher levels of expression in brain and testis (Lehman et al., 1998; Mitsui et al., 1999; Rosa et al., 1996), with the exception of *HERC3*, which is expressed primarily in brain (Davies et al., 2004; Schwarz et al., 1998).

The HERC ligases are localized to the cytoplasm in vesicular-like structures (Garcia-Gonzalo and Rosa, 2005), and are implicated in several physiological functions. *HERC1* has potential oncogenic capacity, as it may have an important role in intracellular membrane trafficking in the Golgi and cytoplasm (Rosa and Barbacid, 1997). Mice deficient for *Herc2* develop *rjs* syndrome (runty, jerky, sterile), which is associated with reduced viability, smaller size, a jerky gait and sterility (Lehman et al., 1998; Rinchik et al., 1995). It has been suggested that the reduced growth and genital hypoplasia observed in *rjs* mice may arise due to neuronal degeneration in the hypothalamus resulting in defective hormonal secretion from the pituitary (Johnson and Hunt, 1975). The functions of HERCs 3 and 5 are not defined (Garcia-Gonzalo and Rosa, 2005), although HERC5 is highly expressed in the testis and ovary, interacts with various cdks (Mitsui et al., 1999) and an increase in its expression is associated with inflammation (Kroismayr et al., 2004; Mitsui et al., 1999).

HERC4 and *HERC6* are the most recently identified forms. An initial characterization revealed that both genes are expressed as multiple spliced products, with higher mRNA levels in brain and testis (Hochrainer et al., 2005). Both are localized to the cytoplasm in vesicular-like structures similar to other HERC family members. The physiological roles of *HERC4* and *HERC6* are unknown.

There is a remarkably high degree of homology among HERC proteins from evolutionarily diverse species, implying that the function(s) of this family of proteins is conserved throughout the animal kingdom (Hochrainer et al., 2005). These facts suggest that the HERC proteins may perform fundamental cellular tasks. The fact that a *HERC4* ortholog is the only *HERC* gene to be found in the nematode genome, strongly suggests that *HERC4* may represent the most ancient family member, from which all others are derived (Hochrainer et al., 2005).

We originally identified *Herc4* as a gene whose expression was upregulated in the luminal epithelium of the mouse uterus at the time of blastocyst implantation and we wished to determine whether *Herc4* expression was essential to normal reproduction. Here we show that the disruption of the murine *Herc4* gene does not affect female reproduction; however, disruption results in a reduction in male fertility associated with a defect in the late stages of spermiogenesis. These results identify for the first time a function for the most ancient member of the HERC family.

Materials and methods

Generation of mutant mice

The mouse ES cell clone RRH224 (strain 129/Ola), with an insertional gene-trap mutation in *Herc4*, was obtained from BayGenomics (http://baygenomics.ucsf.edu/). The gene-trapping vector, pGT2Lxf, was inserted into intron 13, predicting to yield a fusion transcript containing exons 1–13 of *Herc4* upstream of *β-geo*. The ES cells were injected into C57BL/6$^{cBrd/cBrd/Cr}$ blastocysts (Stewart, 1993). Germ line transmission of the targeted *Herc4* allele was determined by PCR and Southern analysis of genomic DNA isolated from tail biopsies. Heterozygous mice (*Herc4*$^{+/β\text{-}geo}$) were intercrossed to obtain homozygous mutant mice (*Herc4*$^{β\text{-}geo/β\text{-}geo}$).

Fertility

To quantify *Herc4*$^{+/+}$ and *Herc4*$^{β\text{-}geo/β\text{-}geo}$ male fertility, each male was mated with females of proven fertility. Females were checked for a vaginal plug the next day. Mated females were moved to a separate cage and replaced with fresh females so that each male had mated with a total of 5–6 females. The mated females were sacrificed at day 9 of pregnancy and the number of implantation sites and embryos counted.

Northern analysis

Total RNA from wild-type and *Herc4*$^{β\text{-}geo/β\text{-}geo}$ mutant mice was isolated using the RNeasy system (Qiagen). 10 μg of each sample were analyzed by Northern analysis (Sambrook et al., 1989) transferred to Hybond-N^{+} membranes (Amersham Pharmacia, Uppsala, Sweden), hybridized with ^{32}P-labeled cDNA probes using ExpressHyb Hybridization solution (Clontech). Mouse adult tissue blots were from Seegene USA (Rockville MD).

β-Galactosidase staining

Tissues were fixed in 0.2% glutaraldehyde, 5 mM EGTA, 2 mm $MgCl_2$ and 0.1 M Na-phosphate buffer (pH 7.3); permeabilized in 0.01% Na-deoxycholate, 0.02% NP-40, 2 mM Mg Cl_2 and 0.1 M Na-phosphate buffer (pH 7.3); and incubated in X-Gal solution (2 mM $MgCl_2$, 5 mM potassium ferricyanide, 5 mM potassium ferrocyanide, and 1 mg/ml X-Gal 5-bromo-4-chloro-3-indolyl-β-D-galactosidase). Cryosections were from excised tissues washed in phosphate-buffered saline (PBS) at 4 °C in formaldehyde, 5 mM EGTA/2 mM $MgCl_2$.

Following incubation overnight in 18% sucrose, the tissues embedded in Tissue Tek were sectioned at 10 μm, dried, fixed, washed in PBS and incubated in X-Gal solution overnight at 30 °C and counterstained with neutral red.

Spermatozoa analysis

Mature male mice were sacrificed by CO_2 asphyxiation, the caudae epididymides and vas deferentia removed, cut into small pieces, transferred to culture medium and incubated for 5 min at RT. Spermatozoon concentration was assessed by counting a 3-μl sample in a microcell. Spermatozoon motility was also assessed based on the number of moving cells versus immotile cells using standardized criteria (WHO, 1992). An average from all fields observed was used to calculate a percentage of motile spermatozoa. The quality of motion (progressive motility) for each spermatozoon was judged by observing the following: (1) the straight or meandering path for individual spermatozoa; (2) the forward or stationary (in place) movement; and (3) the speed (per spermatozoa), i.e. fast, average, slow. The scoring system was 0 to 4. Spermatozoan morphology (angulated tails) was assessed by examining ~100 spermatozoa.

Scanning electron microscopy (SEM)

Spermatozoa suspensions were fixed in of 8% formaldehyde and 4% glutaraldehyde in 0.1 M Na cacodylate buffer pH 7.4. Equal volumes of the spermatozoan suspension and fixative were added and incubated overnight at 4 °C, the solution removed by filtering through a 0.45-μm nylon filter, and washed twice with 0.1 M Na cacodylate buffer. The filter and attached spermatozoa were post-fixed with 1% OsO_4 for 1 h at RT, washed 3× with cacodylate buffer, dehydrated in a graded ethanol series, immersed 3× in tetramethylsilane, and air-dried at room temperature. The filter pieces were mounted and the samples coated with gold–palladium under vacuum (Denton DV-502a). Spermatozoa were photographed with a Hitachi S-3000N SEM at 10 kV (Gonda et al., 1976).

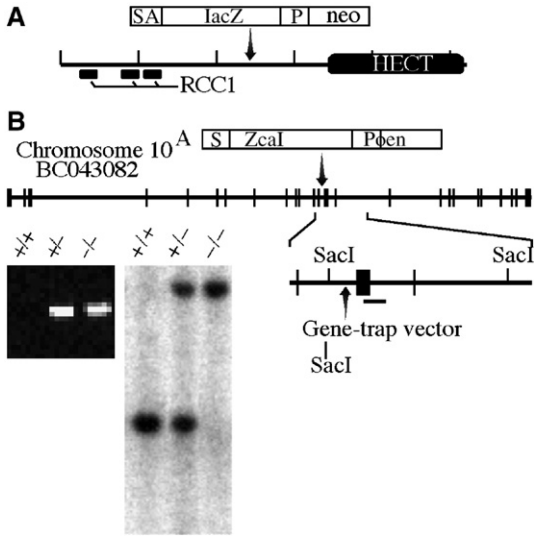

Fig. 1. Generation of *Herc4*$^{β\text{-}geo/β\text{-}geo}$ mice. (A) Mapping of the gene-trap insertion in the *Herc4* gene. (B) Genotyping of wild-type, *Herc4*$^{β\text{-}geo/+}$ and *Herc4*$^{β\text{-}geo/β\text{-}geo}$ mice by Southern analysis and by PCR. The 25 exons of *Herc4* are shown. The gene-trap cassette is inserted into intron 13 and introduced a new *Sac*I restriction site. Southern blot genotyping of progeny derived from an intercross of *Herc4*$^{β\text{-}geo/+}$ heterozygous mice. Genomic DNA was digested with *Sac*I and Southern blotted with 457 bp probe derived from a region located in part of the exon 13 and intron 14. Primers inside the *β-geo* resistance cassette were used to confirm the location of the *neo*^{r} gene insertion.

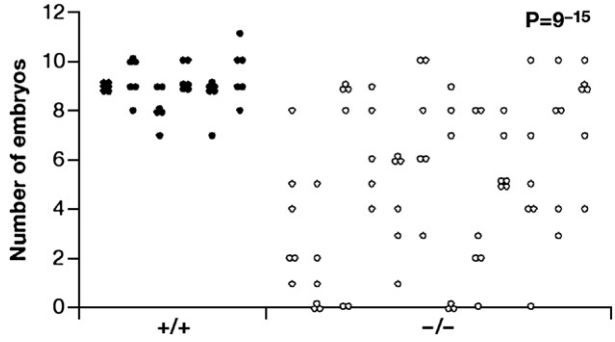

Fig. 2. *Herc4* is essential for normal male fertility. Wild-type females were mated with either wild-type or *Herc4*$^{β\text{-}geo/β\text{-}geo}$ males. Nine days after mating the females were sacrificed and the number of embryos counted. Each column represents the numbers of embryos in each pregnancy produced by a single male. A column of filled dots represents the number of embryos obtained from an individual wild-type male and open dots represent the embryos obtained from individual *Herc4*$^{β\text{-}geo/β\text{-}geo}$ male mice. The overall numbers of embryos produced by the two groups is significantly different with a P value of 9×10^{-15}.

Transmission electron microscopy (TEM)

Spermatozoa were fixed as for SEM, and a portion pelleted by centrifugation. The pellet was rinsed in cacodylate buffer and post fixed in 1% osmium tetroxide 1 h/RT, washed 2× with cacodylate buffer pH 7.4 and 1× with acetate buffer, stained with 0.5% uranyl acetate 1 h/RT, washed 2× with acetate buffer, dehydrated in ethanol, then 100% propylene oxide, and then infiltrated in 100% propylene oxide and epoxy resin. The pellet was embedded in epoxy resin and cured at 55 °C for 48 h. The embedded pellet was sectioned at 60–90 nm. The thin sections were mounted and stained in uranyl acetate and lead citrate. Images were digitally recorded using a Hitachi 7000 electron microscope at 75 kV (Gonda et al., 1976).

Results

Identification and disruption of the Herc4 gene in mice

We originally identified *Herc4* (BC043082) as an uncharacterized cDNA whose expression was upregulated in the uterine luminal epithelium at the time of embryo implantation (data not shown). Subsequent analysis revealed the cDNA corresponds to that transcribed from the *Hect4* gene. *Herc4* cDNA encodes a peptide of 1049 amino acids. It contains one HECT domain and three RLD domains (Hochrainer et al., 2005).

An ES cell clone (RRH224) with a gene-trap vector insertion in intron 13 of the *HERC4* gene was identified in the BayGenomics database (http://baygenomics.ucsf.edu/). The fusion transcript of this clone contained the three RLDs but lacked the HECT domain (Fig. 1A). We used the ES clone to derive mice deficient in *Herc4* to determine the function of this novel E3 ligase in murine development and reproduction. Germ line-transmitting chimeras yielded *Herc4* heterozygotes, which were intercrossed to produce progeny of all three genotypes (Fig. 1B). Homozygous *Herc4*$^{β\text{-}geo/β\text{-}geo}$ mice were viable and indistinguishable from their wild-type littermates. Both male and female *Herc4*$^{β\text{-}geo/β\text{-}geo}$ mice grew normally and had no obvious morphological or behavioral differences (data not shown).

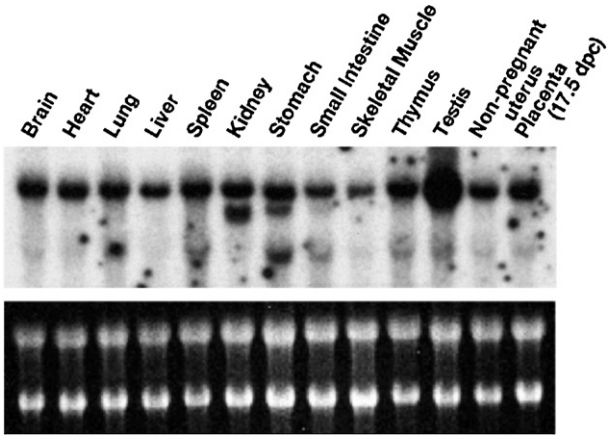

Fig. 3. *Herc4* is highly expressed in testis. Northern blot analysis of multiple mouse tissues showed that *Herc4* transcripts are expressed in all tissues tested, with the strongest expression in the testis. Alternatively spliced transcripts were detected in some tissues (spleen, stomach, kidney, and small intestine) but at a lower levels of expression. The lower panel shows the rRNA levels as a loading control.

Herc4$^{\beta\text{-}geo/\beta\text{-}geo}$ male mice have a fertility defect

We noted, however, that *Herc4$^{\beta\text{-}geo/\beta\text{-}geo}$* males produced significantly smaller numbers of offspring compared to wild-type littermates, suggesting a reproductive defect in the mutant mice. In contrast, *Herc4$^{\beta\text{-}geo/\beta\text{-}geo}$* females had normal fertility and litter sizes. To quantify this reduction in fertility, we mated *Herc4$^{\beta\text{-}geo/\beta\text{-}geo}$* males with females of proven fertility. Nine days later, the females were sacrificed and the number of embryos in the uteri was counted. The mean number of embryos produced by twelve *Herc4$^{\beta\text{-}geo/\beta\text{-}geo}$* males varied widely (5.12±5). This mean number was significantly smaller than the mean number produced by six *Herc4$^{+/+}$* males (9.25±2) ($p \geq 9 \times 10^{-15}$). Some mutant males showed reduced fertility rates slightly lower than heterozygotes and/or wild-type males, while other mutant males were almost completely infertile (Fig. 2). No differences were observed in the mating behavior of *Herc4$^{\beta\text{-}geo/\beta\text{-}geo}$* males and their wild-type littermates, since the time that they took to mate, as assessed by plugging frequency, with females was similar between all male genotypes (data not shown).

Herc4 is highly expressed in the testis

Northern blot analysis on total RNA from multiple tissues revealed that the *Herc4* mRNA is ubiquitously expressed in all tissues examined (Fig. 3). Additional smaller transcripts were also detected in the kidney and stomach, which is consistent with the existence of alternately spliced *Herc4* transcripts (Hochrainer et al., 2005). The highest expression for the largest transcript was observed in the testis, where *Herc4* expression was 4–5 times higher than in other tissues (Fig. 3).

To confirm gene targeting, Northern blot analysis of mouse testes was performed using RNA from *Herc4$^{+/+}$*, *Herc4$^{+/\beta\text{-}geo}$* and *Herc4$^{\beta\text{-}geo/\beta\text{-}geo}$* mice. When the Northern blot was probed with a cDNA fragment 3′ to the *β-geo* insertion, *Herc4* mRNA levels were reduced in the testes of *Herc4$^{+/\beta\text{-}geo}$* mice and undetectable in *Herc4$^{\beta\text{-}geo/\beta\text{-}geo}$* mice, confirming the targeted inactivation of *Herc4* (Fig. 4A, upper panel). A hybridization probe to a region upstream of the insertion site revealed the presence of a novel higher molecular weight mRNA of the targeted *Herc4* mutant allele, that replaced the mRNA signal of

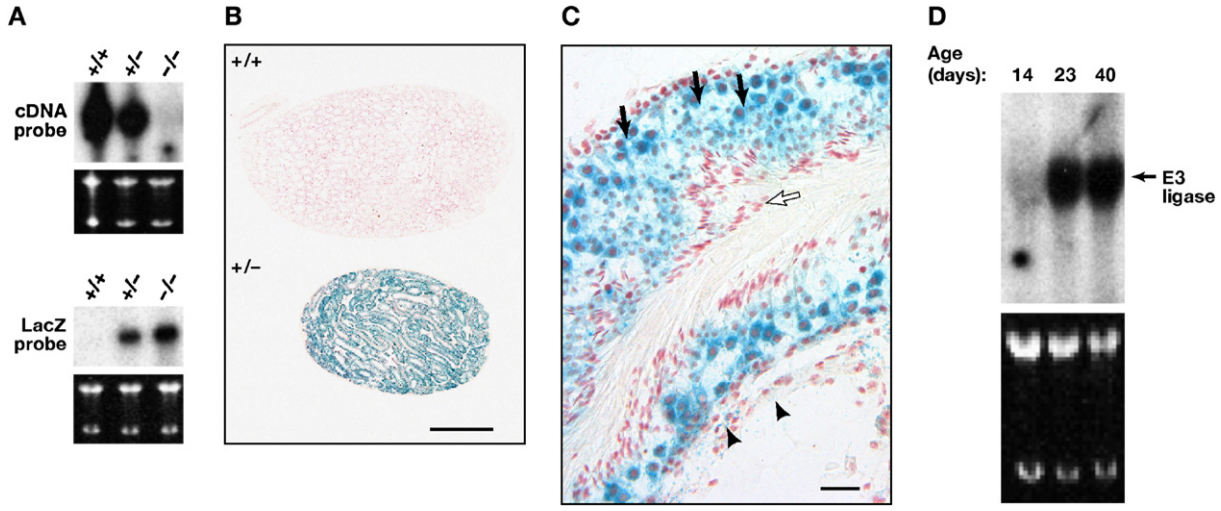

Fig. 4. Expression of mutant and wild-type *Herc4* in the testis. Northern blot analysis was performed to confirm the absence of the wild-type transcript in the testis of *Herc4$^{\beta\text{-}geo/\beta\text{-}geo}$* mice. (A; upper panel) 10 μg of RNA isolated from adult testis from wild-type, *Herc4$^{\beta\text{-}geo/+}$* and *Herc4$^{\beta\text{-}geo/\beta\text{-}geo}$* were hybridized with a probe containing the *Herc4* cDNA (3282–4016 bp) where the endogenous transcript of 4 kb is detected only in the wild-type and heterozygous samples. rRNA loading controls are also shown (lower panel). The *LacZ* probe detected the expected fusion transcripts of 6.8–7 kb mRNA in the *Herc4$^{\beta\text{-}geo/+}$* and *Herc4$^{\beta\text{-}geo/\beta\text{-}geo}$* mice. (B) β-Galactosidase activity in *Herc4$^{\beta\text{-}geo/+}$* mice detected by X-Gal staining of testes sections. (C) β-Galactosidase-stained testis section of adult *Herc4$^{\beta\text{-}geo/+}$* mouse showing strong cytoplasmic expression in virtually all stages of spermatogenesis (filled arrows) with the exception of the spermatozoa (white arrow) and interstitial cells (arrow heads) (scale bar=25 μm). (D) Northern blot analysis of RNA (10μg) isolated from testis of wild-type and *Herc4$^{\beta\text{-}geo/\beta\text{-}geo}$* animals showed almost undetectable expression levels of *Herc4* at P14 after birth. High levels of *Herc4* were detected using a cDNA probe from P20 onward, when spermiogenesis is initiated.

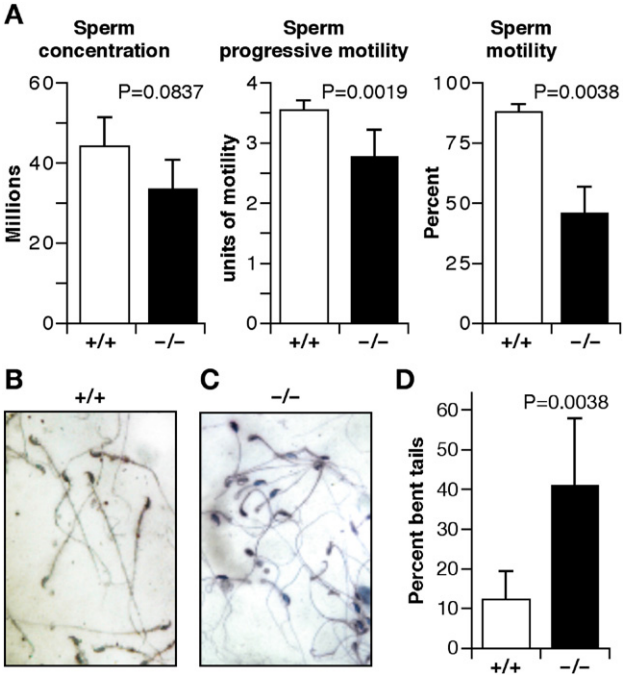

Fig. 5. Functional analysis of spermatozoa from wild-type and *Herc4*$^{\beta\text{-}geo/\beta\text{-}geo}$ mice. (A) Analyses were performed on spermatozoa from three wild-type and eight *Herc4*$^{\beta\text{-}geo/\beta\text{-}geo}$ mice. The differences in spermatozoa concentration levels were not significant between the two genotypes ($P=0.0837$). In contrast, both progressive motility (as assigned on a point basis – see Materials and methods) and total mobility parameters of spermatozoa were significantly decreased in *Herc4*$^{\beta\text{-}geo/\beta\text{-}geo}$ animals. Representative wild-type (B) and *Herc4*$^{\beta\text{-}geo/\beta\text{-}geo}$ spermatozoa (C) stained with periodic acid-Schiff are shown with wild-type spermatozoa showing straight flagella. *Herc4*$^{\beta\text{-}geo/\beta\text{-}geo}$ spermatozoa showed a high proportion with bent tails. (D) Percentage of angulated tails observed in spermatozoa of wild-type (+/+) and *Herc4*$^{\beta\text{-}geo/\beta\text{-}geo}$ adult animals (counts were obtained from three wild-type and eight *Herc4*$^{\beta\text{-}geo/\beta\text{-}geo}$ mice).

the wild-type *Herc4* allele (Fig. 4A, lower panel). This band coincided with the signal obtained with a *lacZ* cDNA probe that was exclusively detected in the targeted *Herc4* mutant but not in the wild-type *Herc4* mice (Fig. 4B). These results demonstrate efficient expression of the *lacZ* reporter gene under the control of the *Herc4* promoter. We then confirmed, by whole-mount X-Gal staining for *lacZ* reporter gene activity, strong expression of the transcripts in *Herc4*$^{+/\beta\text{-}geo}$ testes. Stronger β-galactosidase staining was observed in the testes from *Herc4*$^{\beta\text{-}geo/\beta\text{-}geo}$ littermates and was absent in *Herc4*$^{+/+}$ littermates, confirming the specificity of the staining (Fig. 4B and data not shown).

Herc4 expression is upregulated during spermatogenesis

To determine the onset of *Herc4* expression during spermatogenesis, juvenile wild-type male mice were analyzed during puberty. In mice, the first wave of spermatogenesis begins shortly after birth, and the first meiotic divisions occur at about postnatal day 20 (P20) and by P35 the first spermatozoa are produced (McCarrey, 1993). At the mRNA level, *Herc4* expression was almost undetectable in testes at P14. However, by P23, a strong increase in *Herc4* mRNA levels was observed with expression persisting to P40 when spermatozoa were first observed (Fig. 4D).

To identify the cell type(s) expressing Herc4 protein, β-galactosidase staining for *lacZ* reporter gene activity was performed on *Herc4*$^{\beta\text{-}geo/+}$ testis cryosections (Fig. 4C). All stages of spermatogenesis were present, and the staining revealed *lacZ* reporter gene activity in spermatogonia, spermatocytes, and spermatids with little or no activity detectable in the spermatozoa, or interstitial cells.

Herc4$^{\beta\text{-}geo/\beta\text{-}geo}$ *males display reduced spermatozoon motility and a high percentage of spermatozoa having an angulated tail*

Although the size and morphology of *Herc4*$^{\beta\text{-}geo/\beta\text{-}geo}$ adult testes appeared normal (data not shown), the expression pattern of *Herc4* at different stages of spermatogenesis coupled with the reduced fertility of the mutant males suggested that the defects were present at the cellular level. The *Herc4*$^{\beta\text{-}geo/\beta\text{-}geo}$ males did not show any significant differences compared to the wild-type animals with respect to spermatozoon count (Fig. 5A) in isolates from the caudea epididymes and vas deferens. However, a

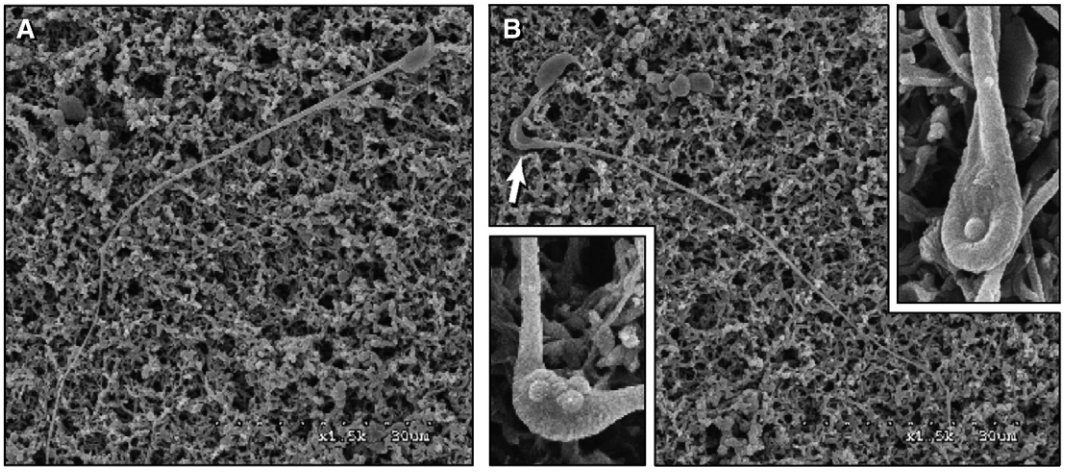

Fig. 6. *Herc4* mutants displayed marked flagellar angulation. SEM microscopy of a normal spermatozoa flagellum (A) in contrast to the bent flagellum in *Herc4*$^{\beta\text{-}geo/\beta\text{-}geo}$ spermatozoa (B). The arrow indicates the protuberance on the spermatozoa tail. Insets show two examples of protuberances at higher magnification. Images shown are representative of spermatozoa from 3 animals/each genotype.

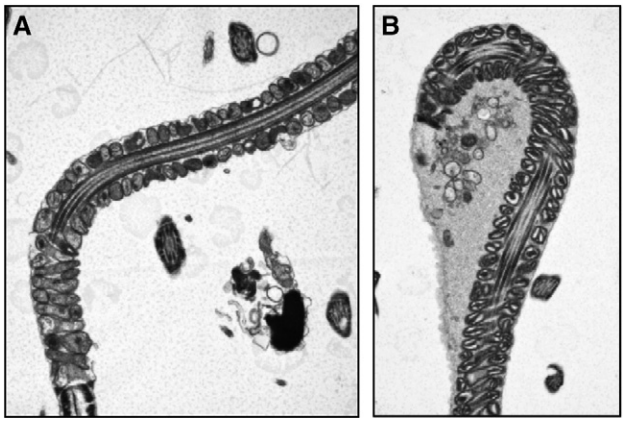

Fig. 7. Retention of the cytoplasmic droplet at the angulation. TEM microscope analysis showing a mature flagellum of a wild-type spermatozoon (A) in comparison with an age-matched *Herc4*$^{\beta\text{-}geo/\beta\text{-}geo}$ flagellum with the cytoplasmic droplet containing many degraded organelle membranes (B).

significant motility defect was found in *Herc4*$^{\beta\text{-}geo/\beta\text{-}geo}$ spermatozoa compared to those from wild-type mice. The rate at which the spermatozoa moved forward (spermatozoon progressive motility) as well as spermatozoon motility was decreased by about 50% in mutant animals compared to wild-type littermates (Fig. 5A).

The reduction in spermatozoon motility correlated with a high percentage of *Herc4*$^{\beta\text{-}geo/\beta\text{-}geo}$ spermatozoa showing a specific tail abnormality. *Herc4*$^{\beta\text{-}geo/\beta\text{-}geo}$ mice had a three fold higher proportion of angulated tails than wild-type animals (Figs. 5B and C). Scanning electron microscopy revealed that the mutant spermatozoa contained a cytoplasmic droplet attached to the flagellum at the point in which the flagellum exhibited a marked angulation (Fig. 6B). These cytoplasmic droplets were absent in wild-type spermatozoa, which had a straight flagellum (Fig. 6A).

TEM analysis of the mutant spermatozoa flagella revealed the cytoplasmic droplet contained large amounts of residual cytoplasm, often with dilated mitochondria and vacuoles. These resembled the cytoplasmic droplets present in the epididymal spermatozoa, suggesting that separation of the cytoplasmic droplets from the developing spermatozoa (Figs. 7A and B) failed.

Discussion

The components of the ubiquitin–proteasome system are expressed in all cell types and have essential roles in regulating the levels of a variety key proteins essential to fundamental cellular processes, such as receptor internalization, trafficking, signal transduction, cell cycle, apoptosis and DNA repair (Glickman and Ciechanover, 2002; Muratani and Tansey, 2003; Varshavsky, 2005; Wilkinson, 2000). Spermatogenesis is also dependent on the ubiquitin system (Sutovsky, 2003), as exemplified by the first knockout for a component of the ubiquitin pathway (the ubiquitin-conjugating enzyme, HR6B) resulting in males that were infertile due to defective spermatogenesis (Roest et al., 1996). In humans, teratozoospermic individuals show extensive disruption in RNA expression profiles of the ubiquitin–proteasome pathway (Platts et al., 2007) and a mutation in a deubiquitination gene, *USP9Y*, affects spermatogenesis with no apparent effect on somatic tissues (Sun et al., 1999).

Mammalian spermatogenesis involves the differentiation of diploid spermatogonia into spermatocytes and then, through two successive meiotic divisions, into round haploid spermatids. During spermiogenesis, the round haploid spermatids undergo an elongation phase, transforming them into mature spermatozoa. Defects in these processes lead to a lack of mature spermatozoa (azoospermia) and is a major cause of male infertility in the human population (Ezeh, 2000).

Different stages of spermatogenesis require specialized activities of the ubiquitin pathway. During spermiogenesis in particular, the general activity of the ubiquitin pathway is high, possibly due to the extensive degradation of cytoplasmic and nuclear proteins required during the last phase of spermatogenesis (Baarends et al., 2000). The reduction of spermatozoon cytoplasmic volume and destruction of organelles during spermiogenesis is achieved by the removal of the last portion of male germ cell cytoplasm, the spermatozoon cytoplasmic droplet. The spermatozoon cytoplasmic droplet (CD) is composed of cytosol and organelle-derived membranes, which are thought to be the remnants of Golgi and other spermatid organelles degraded during the final stages of spermiogenesis (Oko et al., 1993). Ubiquitination is present in the CD (Kuster et al., 2004), with a ubiquitin-specific processing protease also being present in the CD (Baarends et al., 2000).

Other members of the ubiquitin pathway are also associated with spermatogenesis (Sutovsky, 2003), and recently a novel testis E3 ligase containing a HECT domain, was isolated suggesting a potential role in chromatin condensation during spermatid maturation (Liu et al., 2005). Here we show that a gene-trap insertion into the murine E3 ligase *Herc4* that produces a fusion transcript containing the first 12 exons of the *Herc4* gene joined the *β-geo* marker resulting in a reduction in male fertility. The fusion transcript contains the RLDs of *Herc4*, but lacks the HECT domain, which is the structural domain required for ubiquitin ligase function. *Herc4*$^{\beta\text{-}geo/\beta\text{-}geo}$ mice are overtly normal and healthy with no obvious morphological or behavioral differences apart from a clear reduction in male fertility. The smaller litter sizes produced by *Herc4*$^{\beta\text{-}geo/\beta\text{-}geo}$ males compared with the litter sizes of wild-type counterparts are consistent with the high level of expression and functional activity of *Herc4* in the adult testis (4- to 5-fold higher compared to the twelve other mouse tissues tested). However, there was a wide variability both between individual males and within specific males themselves with regard to the numbers of offspring resulting from each mating. The cause(s) of this variation are unclear, although there was significant variation in the numbers of spermatozoa with angulated tails with all *Herc4*$^{\beta\text{-}geo/\beta\text{-}geo}$ males (Fig. 5D) tested suggesting a correlation between numbers of offspring and misshapen spermatozoa. It may be possible that other Herc ubiquitin ligases that are expressed in the testis may be

compensating for loss of Herc4. This will, however, have to be resolved once mouse lines deficient in other *Herc* genes become available.

Herc4 E3 ligase is expressed in the cytoplasm of spermatogonia, spermatocytes, and spermatids, but is not detectable in elongating spermatids or interstitial cells of the testis. These patterns of expression strongly suggest an important role for *Herc4* during spermatogenesis. These data were supported by Northern blot studies in which *Herc4* mRNA was almost undetectable in the first stages of juvenile spermatogenesis, but was strongly expressed in later stages of spermatogenesis (McCarrey, 1993). In accordance with these data, a marked defect in the morphology of the flagellum was detected by scanning electron microscopy, which showed a high percentage of angulated spermatozoan tails in mutant animals compared to wild-types. The angulated spermatozoan tails showed a protuberance attached to each flagellum, which impaired the movement of the spermatozoa, resulting in reduced motility and a slower rate of progressive motility. Transmission electron microscopy showed that the contents of the protuberance were consistent with the residual cytoplasm observed in the CD (Oko et al., 1993). Retention of the CD is associated with spermatozoa being functionally deficient at fertilization (Thundathil et al., 2001).

It is not clear how loss of *Herc4* resulted in the retention of the cytoplasmic droplet and bending of the flagellum. Most studies on ubiquitination during spermiogenesis have focused on changes in chromatin composition and on organelle (mitochondrial) removal and remodelling. However, a reassessment of the first targeted ubiquitin (*Ube2b*) mutation in mice (Roest et al., 1996) indicated that apart from the defects described in the nucleus, loss of *Ube2b* also disrupted assembly of flagellar structures (Escalier et al., 2003). Our results suggest that *Herc4* functions as an ubiquitin ligase involved in either protein trafficking or in the distribution of cellular structures rather than their degradation.

Intriguingly, at least three other lines of mice have been derived which exhibit male specific infertility, which is associated with angulation of the flagellum similar to the phenotype described here. Mice deficient in either the orphan receptor tyrosine kinase *c-ros*, or *Spem1* that encodes a protein of unknown function are infertile (Sonnenberg-Riethmacher et al., 1996; Zheng et al., 2007). Similarly, mice carrying the transgene insertion GPX5-Tag2 are also infertile (Sipila et al., 2002). Spermatozoa from all three lines show angulation of the flagellum and retention of the CD, although the lines differ in their ability to fertilize eggs *in vitro* (Cooper et al., 2004). In the testis, *c-ros* expression is restricted to the initial segment of the caput epididymides and both the *c-ros*-deficient mice and the GPX5-Tag2 exhibit an abnormal epididymides (Cooper et al., 2004). Clearly, the molecular basis to how angulation of the flagellum arises is complex, involving both cell autonomous factors (*Herc4* and *Spem1*) and possibly environmental effects (*c-ros* and GPX5-Tag2).

The identification of *Herc4* as an E3 ubiquitin ligase, the expression pattern (human and murine testes) of *Herc4* and male fertility defects in $Herc4^{\beta\text{-}geo/\beta\text{-}geo}$ mice support a specific role for this gene during spermiogenesis. *Herc4* is expressed at lower levels in several mouse tissues other than the testis. This expression pattern is in agreement with the higher levels of human *HERC4* mRNA expression in brain and testis (Hochrainer et al., 2005). The subcellular localization of human HERC4 protein showed a cytoplasmic pattern similar to that observed in the mouse in various stages of male germ cell development (Hochrainer et al., 2005). There is also a high degree of homology between the human and mouse HERC ligases with 91% identity at the nucleotide level and 93% identity to the mouse ortholog (Garcia-Gonzalo and Rosa, 2005). Taken together, the sequence conservation and our data showing that the $Herc4^{\beta\text{-}geo/\beta\text{-}geo}$ mice display a marked flagellar defect strongly suggest that *HERC4* may play a significant role in human spermiogenesis, although there is no published evidence that male infertility is linked to the chromosomal region 10q22, where *HERC4* is located.

Herc4 is necessary for proper spermiogenesis and male fertility in mice. Because the physiological role of *Herc4* in spermiogenesis may be conserved in other mammalian species, including humans, an understanding of its cellular function in mice may help elucidate the molecular basis for some cases of infertility in men.

Acknowledgments

We are very grateful to Roakie Awashti for help in the fertility assays, Kunio Nagashima for the EM images and Richard Frederickson, for help in preparation of the figures. This research was supported by the Intramural Research Program of the NCI.

References

Baarends, W.M., Roest, H.P., Grootegoed, J.A., 1999. The ubiquitin system in gametogenesis. Mol. Cell. Endocrinol. 151, 5–16.

Baarends, W.M., van der Laan, R., Grootegoed, J.A., 2000. Specific aspects of the ubiquitin system in spermatogenesis. J. Endocrinol. Invest. 23, 597–604.

Ciechanover, A., Orian, A., Schwartz, A.L., 2000. Ubiquitin-mediated proteolysis: biological regulation via destruction. BioEssays 22, 442–451.

Cooper, T.G., Yeung, C.H., Wagenfeld, A., Nieschlag, E., Poutanen, M., Huhtaniemi, I., Sipila, P., 2004. Mouse models of infertility due to swollen spermatozoa. Mol. Cell. Endocrinol. 216, 55–63.

Davies, W., Smith, R.J., Kelsey, G., Wilkinson, L.S., 2004. Expression patterns of the novel imprinted genes *Nap1l5* and *Peg13* and their non-imprinted host genes in the adult mouse brain. Gene Expr. Patterns 4, 741–747.

de Kretser, D.M., Loveland, K.L., Meinhardt, A., Simorangkir, D., Wreford, N., 1998. Spermatogenesis. Hum. Reprod. 13 (Suppl. 1), 1–8.

Escalier, D., Bai, X.Y., Silvius, D., Xu, P.X., Xu, X., 2003. Spermatid nuclear and sperm periaxonemal anomalies in the mouse *Ube2b* null mutant. Mol. Reprod. Dev. 65, 298–308.

Ezeh, U.I., 2000. Beyond the clinical classification of azoospermia: opinion. Hum. Reprod. 15, 2356–2359.

Garcia-Gonzalo, F.R., Rosa, J.L., 2005. The HERC proteins: functional and evolutionary insights. Cell. Mol. Life Sci. 62, 1826–1838.

Glickman, M.H., Ciechanover, A., 2002. The ubiquitin–proteasome proteolytic pathway: destruction for the sake of construction. Physiol. Rev. 82, 373–428.

Gonda, M.A., Aaronson, S.A., Ellmore, N., Zeve, V.H., Nagashima, K., 1976. Ultrastructural studies of surface features of human normal and tumor cells

in tissue culture by scanning and transmission electron microscopy. J. Natl. Cancer Inst. 56, 245–263.

Hershko, A., Ciechanover, A., Varshavsky, A., 2000. Basic medical research award. The ubiquitin system. Nat. Med. 6, 1073–1081.

Hochrainer, K., Mayer, H., Baranyi, U., Binder, B., Lipp, J., Kroismayr, R., 2005. The human HERC family of ubiquitin ligases: novel members, genomic organization, expression profiling, and evolutionary aspects. Genomics 85, 153–164.

Ji, Y., Walkowicz, M.J., Buiting, K., Johnson, D.K., Tarvin, R.E., Rinchik, E.M., Horsthemke, B., Stubbs, L., Nicholls, R.D., 1999. The ancestral gene for transcribed, low-copy repeats in the Prader-Willi/Angelman region encodes a large protein implicated in protein trafficking, which is deficient in mice with neuromuscular and spermiogenic abnormalities. Hum. Mol. Genet. 8, 533–542.

Johnson, D.R., Hunt, D.M., 1975. Endocrinological findings in sterile pink-eyed mice. J. Reprod. Fertil. 42, 51–58.

Kroismayr, R., Baranyi, U., Stehlik, C., Dorfleutner, A., Binder, B.R., Lipp, J., 2004. HERC5, a HECT E3 ubiquitin ligase tightly regulated in LPS activated endothelial cells. J. Cell. Sci. 117, 4749–4756.

Kuhne, C., Banks, L., 1998. E3-ubiquitin ligase/E6-AP links multicopy maintenance protein 7 to the ubiquitination pathway by a novel motif, the L2G box. J. Biol. Chem. 273, 34302–34309.

Kumar, S., Talis, A.L., Howley, P.M., 1999. Identification of HHR23A as a substrate for E6-associated protein-mediated ubiquitination. J. Biol. Chem. 274, 18785–18792.

Kuster, C.E., Hess, R.A., Althouse, G.C., 2004. Immunofluorescence reveals ubiquitination of retained distal cytoplasmic droplets on ejaculated porcine spermatozoa. J. Androl. 25, 340–347.

Lehman, A.L., Nakatsu, Y., Ching, A., Bronson, R.T., Oakey, R.J., Keiper-Hrynko, N., Finger, J.N., Durham-Pierre, D., Horton, D.B., Newton, J.M., Lyon, M.F., Brilliant, M.H., 1998. A very large protein with diverse functional motifs is deficient in *rjs* (runty, jerky, sterile) mice. Proc. Natl. Acad. Sci. U. S. A. 95, 9436–9441.

Liu, Z., Oughtred, R., Wing, S.S., 2005. Characterization of E3Histone, a novel testis ubiquitin protein ligase which ubiquitinates histones. Mol. Cell. Biol. 25, 2819–2831.

McCarrey, J.R., 1993. Development of the Germ Cell. Oxford University Press, New York.

Mitsui, K., Nakanishi, M., Ohtsuka, S., Norwood, T.H., Okabayashi, K., Miyamoto, C., Tanaka, K., Yoshimura, A., Ohtsubo, M., 1999. A novel human gene encoding HECT domain and RCC1-like repeats interacts with cyclins and is potentially regulated by the tumor suppressor proteins. Biochem. Biophys. Res. Commun. 266, 115–122.

Muratani, M., Tansey, W.P., 2003. How the ubiquitin–proteasome system controls transcription. Nat. Rev., Mol. Cell Biol. 4, 192–201.

Oda, H., Kumar, S., Howley, P.M., 1999. Regulation of the Src family tyrosine kinase Blk through E6AP-mediated ubiquitination. Proc. Natl. Acad. Sci. U. S. A. 96, 9557–9562.

Oko, R., Hermo, L., Chan, P.T., Fazel, A., Bergeron, J.J., 1993. The cytoplasmic droplet of rat epididymal spermatozoa contains saccular elements with Golgi characteristics. J. Cell Biol. 123, 809–821.

Platts, A.E., Dix, D.J., Chemes, H.E., Thompson, K.E., Goodrich, R., Rockett, J.C., Rawe, V.Y., Quintana, S., Diamond, M.P., Strader, L.F., Krawetz, S.A., 2007. Success and failure in human spermatogenesis as revealed by teratozoospermic RNAs. Hum. Mol. Genet. 16, 763–773.

Rinchik, E.M., Carpenter, D.A., Handel, M.A., 1995. Pleiotropy in microdeletion syndromes: neurologic and spermatogenic abnormalities in mice homozygous for the p6H deletion are likely due to dysfunction of a single gene. Proc. Natl. Acad. Sci. U. S. A. 92, 6394–6398.

Roest, H.P., van Klaveren, J., de Wit, J., van Gurp, C.G., Koken, M.H., Vermey, M., van Roijen, J.H., Hoogerbrugge, J.W., Vreeburg, J.T., Baarends, W.M., Bootsma, D., Grootegoed, J.A., Hoeijmakers, J.H., 1996. Inactivation of the HR6B ubiquitin-conjugating DNA repair enzyme in mice causes male sterility associated with chromatin modification. Cell 86, 799–810.

Rosa, J.L., Barbacid, M., 1997. A giant protein that stimulates guanine nucleotide exchange on ARF1 and Rab proteins forms a cytosolic ternary complex with clathrin and Hsp70. Oncogene 15, 1–6.

Rosa, J.L., Casaroli-Marano, R.P., Buckler, A.J., Vilaro, S., Barbacid, M., 1996. p619, a giant protein related to the chromosome condensation regulator RCC1, stimulates guanine nucleotide exchange on ARF1 and Rab proteins. EMBO J. 15, 4262–4273.

Russell, L., Clermont, Y., 1976. Anchoring device between Sertoli cells and late spermatids in rat seminiferous tubules. Anat. Rec. 185, 259–278.

Sambrook, J., Fritsch, E., Maniatis, T., 1989. Molecular Cloning—A Laboratory Manual. Cold Spring Harbor Laboratory Press, Plainview, NY.

Scheffner, M., Huibregtse, J.M., Vierstra, R.D., Howley, P.M., 1993. The HPV-16 E6 and E6-AP complex functions as a ubiquitin–protein ligase in the ubiquitination of p53. Cell 75, 495–505.

Schwarz, S.E., Rosa, J.L., Scheffner, M., 1998. Characterization of human hect domain family members and their interaction with UbcH5 and UbcH7. J. Biol. Chem. 273, 12148–12154.

Sipila, P., Cooper, T.G., Yeung, C.H., Mustonen, M., Penttinen, J., Drevet, J., Huhtaniemi, I., Poutanen, M., 2002. Epididymal dysfunction initiated by the expression of simian virus 40 T-antigen leads to angulated sperm flagella and infertility in transgenic mice. Mol. Endocrinol. 16, 2603–2617.

Sonnenberg-Riethmacher, E., Walter, B., Riethmacher, D., Godecke, S., Birchmeier, C., 1996. The *c-ros* tyrosine kinase receptor controls regionalization and differentiation of epithelial cells in the epididymis. Genes Dev. 10, 1184–1193.

Stewart, C.L., 1993. Production of chimeras between embryonic stem cells and embryos. Methods Enzymol. 225, 823–855.

Sun, C., Skaletsky, H., Birren, B., Devon, K., Tang, Z., Silber, S., Oates, R., Page, D.C., 1999. An azoospermic man with a de novo point mutation in the Y-chromosomal gene *USP9Y*. Nat. Genet. 23, 429–432.

Sutovsky, P., 2003. Ubiquitin-dependent proteolysis in mammalian spermatogenesis, fertilization, and sperm quality control: killing three birds with one stone. Microsc. Res. Tech. 61, 88–102.

Thundathil, J., Palasz, A.T., Barth, A.D., Mapletoft, R.J., 2001. The use of in vitro fertilization techniques to investigate the fertilizing ability of bovine sperm with proximal cytoplasmic droplets. Anim. Reprod. Sci. 65, 181–192.

Varshavsky, A., 2005. Regulated protein degradation. Trends Biochem. Sci. 30, 283–286.

Weissman, A.M., 2001. Themes and variations on ubiquitylation. Nat. Rev., Mol. Cell Biol. 2, 169–178.

WHO, 1992. Laboratory Manual for the Examination of Human Semen and Sperm–Cervical Mucus Interaction. Cambridge University Press, Cambridge.

Wilkinson, K.D., 2000. Ubiquitination and deubiquitination: targeting of proteins for degradation by the proteasome. Semin. Cell Dev. Biol. 11, 141–148.

Zheng, H., Stratton, C.J., Morozumi, K., Yanagimachi, R., Yan, W., 2007. Lack of *Spem1* causes aberrant cytoplasm removal, sperm deformation, and male infertility. Proc. Natl. Acad. Sci. U. S. A. 104, 6852–6857.